Review of Calculations on Point Defect Properties in Delta-Pu

P. G. Allen, W. G. Wolfer

September 8, 2015

Disclaimer

This document was prepared as an account of work sponsored by an agency of the United States government. Neither the United States government nor Lawrence Livermore National Security, LLC, nor any of their employees makes any warranty, expressed or implied, or assumes any legal liability or responsibility for the accuracy, completeness, or usefulness of any information, apparatus, product, or process disclosed, or represents that its use would not infringe privately owned rights. Reference herein to any specific commercial product, process, or service by trade name, trademark, manufacturer, or otherwise does not necessarily constitute or imply its endorsement, recommendation, or favoring by the United States government or Lawrence Livermore National Security, LLC. The views and opinions of authors expressed herein do not necessarily state or reflect those of the United States government or Lawrence Livermore National Security, LLC, and shall not be used for advertising or product endorsement purposes.

Review of Calculations on Point Defect Properties in δ-Pu

W.G. Wolfer and P. G. Allen

Lawrence Livermore National Laboratory, Livermore, CA

Abstract

The results of theoretical predictions of properties for vacancies and self-interstitial atoms (SIA) in δ-Pu are presented and reviewed. Three methods have been used for these predictions, namely the modified embedded atom method (MEAM), density functional theory (DFT) with and without spin polarization, and continuum mechanics (CM) models adapted to plutonium. The properties considered are formation and migration energies, and relaxation volumes of vacancies and SIA. Predicted values vary considerably. Nevertheless, all three methods predict that the activation energy for self-diffusion by vacancies is of similar magnitude as the SIA formation energy. Furthermore, the absolute magnitudes of relaxation volumes for vacancies and SIA are also similar, indicating that there exist no large bias for radiation-induced void swelling.

Introduction

In each radioactive decay of plutonium, about two to three thousand displacement events occur. The point defects thereby produced, namely vacancies and self-interstitial atoms (SIA), diffuse through the crystal lattice and aggregate to form larger defects. Among these larger defects are numerous helium bubbles in aged δ-Pu [1], but other defects have so far not been found via TEM investigations. This is in contrast to the defect evolution in steels irradiated in nuclear reactors. Here, in addition to voids and bubbles, prismatic dislocation loops are present, and the network dislocation density also changes with radiation exposure. This microstructural evolution depends strongly on the fundamental properties of vacancies and self-interstitial atoms (SIA), and extensive research efforts have been devoted to obtain reliable values for these properties for a few metals, both with experiments and theory. In particular for SIA, experimental approaches are limited, and theoretical investigations have been the dominant avenue to obtain results. These investigations employ empirical interatomic potentials [2], semi-empirical potentials provided by the embedded atom method (EAM) or the modified embedded atom method (MEAM), and lately also ab-initio methods based on density functional theory (DFT). Finally, Wolfer [3] has refined continuum mechanics models to obtain certain properties of vacancies and SIAs in both fcc and bcc metals. All these theoretical approaches have been applied recently to obtain also these properties for point defects in δ-Pu and in gallium-stabilized δ-Pu. The results from these efforts are summarized and compared in this report, and several conclusions are reached to guide future work.

Point Defect Properties based on MEAM.

The development of MEAM potentials of plutonium [4], of gallium [5], as well as of cross potentials for Pu-Ga, Pu-He, and Ga-He interactions [6], has enabled atomistic simulations to determine properties of vacancies, of self-interstitials, and of interstitial and substitutional helium in δ-Pu. Table 1 summarizes results so far obtained.

TABLE 1. Defect formation and migration energies (in eV) obtained with MEAM
in δ-Pu and in Ga-stabilized δ-Pu

Reference	7	6	8	9	10	11	10	13
Material	δ-Pu	Pu 5at.%Ga	δ-Pu	δ-Pu	δ-Pu	δ-Pu	δ-Pu	Pu 5at.%Ga
Vac. formation, E_V^f	0.48				0.44	0.9	0.46	0.58$\pm$0.12
Vac. migration, E_V^m	1.0		1.06		0.8			1.29$\pm$0.30
SIA formation*, E_{SIA}^f					0.49		0.52	1.16$\pm$0.23
SIA migration, E_{SIA}^m	0.056			0.084	0.079			0.4$\pm$0.3
SIA+Vac. formation		1.6						
I-He formation		3.6 unrelaxed				2.3		3.15$\pm$0.51
I-He migration								0.4$\pm$0.2
S-He formation						1.5		
S-He migration								0.9$\pm$0.3
S-He+SIA formation								1.69$\pm$0.70

* for <100> split configuration
I-He is a He atom in an interstitial position, and S-He in a substitutional position

A few observations are noteworthy. First, the vacancy formation energy, E_V^f, is predicted to be significantly smaller than the activation energy for migration, E_V^m, contrary to most other fcc metals. Second, the formation energy of a split <100> self-interstitial is remarkably low; in aluminum with a melt temperature similar to plutonium, this energy is estimated to be 1.82 eV. Third, to place a helium atom into an interstitial site requires a large energy, and as a result, it is predicted to spontaneously produce a Frenkel pair and occupy instead the vacancy; it converts to a substitutional helium because the formation energy of the Pu self-interstitial is so low.

Point Defect Properties based on DFT

Calculations with spin-polarized density-functional theory (SP DFT) have also been attempted, and the results are summarized in Table 2. The predicted vacancy formation energies are excessively large, about as large as experimental values for the self-diffusion energy. In contrast, the formation energy for <100>-split SIA is

remarkably low. This implies that thermally activated production of SIAs is as likely as that of vacancies at microstructural defects such as dislocations, grain boundaries, and helium bubbles.

Another intriguing prediction is the large relaxation of the atoms that surround a vacancy. While in normal fcc metals, the vacancy relaxation volume is around -0.2 Ω, Ω being the atomic volume, the much larger collapse of atoms nearly eliminates the vacancy in δ-Pu.

Table 2. Defect formation and migration energies (in eV) obtained with DFT
for δ-Pu and for Ga-stabilized δ-Pu.

Reference	14	15	16	17	18	19
Material	δ-Pu	δ-Pu	δ-Pu 1.5at.%Ga		δ-Pu	δ-Pu
Method*	SP DFT	SP DFT DM	SP DFT	DFT no SP Pseudo-pot.	SP DFT Plane-wave	SP DFT all electron
Vac. formation, E_V^f	1.5 unrelaxed	1.08 relaxed	1.2		1.35	1.75
Vac. migration, E_V^m	0.85		0.56			
SIA formation*, E_{SIA}^f			0.8 <100> 1.8 <111>		0.73 <100>	
Vac. relaxation, V_V^{rel}/Ω_δ				-0.62	-0.95	-0.7
SIA relaxation, $V_{SIA}^{rel}/\Omega_\delta$				0.40 <100> 0.65 <111>	1.4	

*Split orientation as indicated

Point Defect Properties based on Continuum Mechanics

Vacancy Migration
The atomistic process of vacancy migration consists of one atom next to the vacant site jumping into this site and leaving behind another vacant site. The jump is thermally activated, and transition state theory predicts a diffusion coefficient for vacancy migration in cubic crystals of the form

$$D_V = v_{LV}a^2 \exp(S_V^m/k) \exp(-H_V^m/kT) = D_V^0 \exp(-H_V^m/kT) \qquad (1)$$

Here, v_{LV} is an average frequency for lattice vibrations, a is the lattice parameter, S_V^m is the vacancy migration entropy, and H_V^m is the enthalpy for vacancy migration. It is in fact the energy of an activation barrier that the jumping atom must overcome, and when it temporarily occupies a position at the height of this barrier, the atomic configuration is referred to as the saddle point of the vacancy. It will be considered in greater detail momentarily.

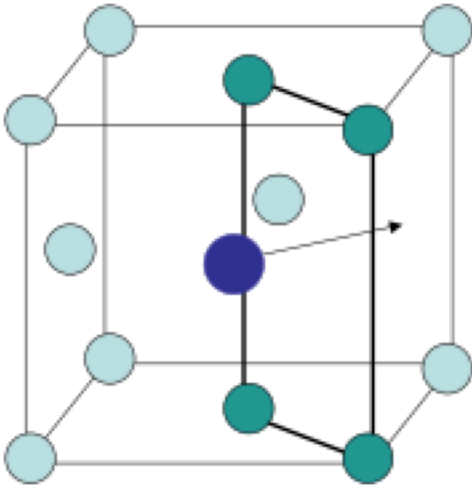Values obtained for H_V^m from experimental measurements for fcc metals increase with the melting point.

Fig. 1. Jump of one nearest-neighbor atom of a vacancy through a cannel formed by four atoms.

The saddle-point configuration of the vacancy involves not just the displacement of the jumping atom, but also the coordinated motion of other atoms that are nearest neighbors of the vacancy and of the jumping atom. These nearest neighbor atoms lie at the corners of a rectangular plane as shown in Figure 1, and as the jumping atom crosses this plane, they are displaced such that it opens the channel. This coordinated motion can be viewed as a particular strain fluctuations and described in terms of phonon excitations. In this manner, Flynn [20] has derived the following formula for the energy of vacancy migration in cubic crystals.

$$E_V^m = \frac{15 C_{11} C_{44} (C_{11} - C_{12}) a^3 \chi}{2 \left[C_{11}(C_{11} - C_{12}) + C_{44}(5C_{11} - 3C_{12}) \right]} \quad Joule \qquad (2)$$

Here, a is the lattice parameter and χ is an empirical parameter that characterizes the shape of the activation barrier and can be determined by comparing experimental vacancy migration energies with values predicted by equation (2). Ehrhart et. al [21] recommend that $\chi = 0.022$ for fcc metals.

In the derivation of Flynn, only the four nearest neighbor atoms are supposed to move, while all other atoms are assumed to remain in their normal lattice positions. On the other hand, Kornblit et al.[22] treat the expansion of the diffusion channel as a quasi-static elastic deformation of the entire surrounding material. The extent of the expansion is such that the opened channel is equal to the cross-section of the jumping atom, and the linear anisotropic elasticity calculation is carried out by a variational method. A vacancy migration energy for fcc metals of

$$E_V^m = 0.0010776 \, a^3 \, p_0 \frac{p_0 p_1 - p_2^2}{p_0^2 + \frac{2}{9} p_0 p_2 + \frac{1}{9} p_2^2} \quad eV \tag{3}$$

is obtained, and the parameters p_i are linear functions of the three elastic constants.

$$p_0 = 5.29833 \, C_{11} - 4.76499 \, C_{12} + 9.35238 \, C_{44}$$

$$p_1 = 0.86667 \, C_{11} - 0.33330 \, C_{12} + 1.91111 \, C_{44}$$

$$p_2 = 1.41903 \, C_{11} - 0.88570 \, C_{12} + 1.64444 \, C_{44}$$

The self-diffusion coefficient determines the transport of atoms through the crystal under conditions near the thermodynamic equilibrium, and it is defined as

$$D_{SD} = D_V^m \, C_V^{eq} = \nu_{LV} a^2 \exp((S_V^f + S_V^m)/k) \exp(-Q_{SD}/kT) = D_{SD}^0 \exp(-Q_{SD}/kT) \tag{4}$$

where the activation energy for self-diffusion is

$$Q_{SD} = E_V^f + E_V^m. \tag{5}$$

The most accurate measurements of diffusion coefficients is done with a radioactive tracer isotope of the metal under investigation, and in this case one obtains values for the tracer self-diffusion coefficient

$$D_{SD}^T = f \, D_{SD}$$

that involves the correlation factor f. For pure elemental metals of cubic structure, f is a constant and can be determined exactly by computation. For fcc crystals, $f = 0.78145$. To determine then the pre-exponential factor for self-diffusion

$$D_{SD}^0 = \nu_{LV} \, a^2 \exp((S_V^f + S_V^m)/k) \tag{6}$$

requires values for the entropy $S_V^f + S_V^m$ and for the attempt frequency ν_{LV}. Based on theoretical estimates, Seeger and Mehrer [23] recommend a value of 2.5 k for the former. The atomic vibration of nearest neighbor atoms to the vacancy is treated within a

sinusoidal potential energy profile that has a maximum height of E_V^m. For small-amplitude vibrations the attempt frequency is then given by

$$\nu_{LV} = \frac{1}{a}\sqrt{\frac{E_V^m}{M}} \tag{7}$$

where M is the atomic mass. Table 3 provides the vacancy migration properties for the two Ga-stabilized δ-Pu alloys for which single crystal elastic constants are available [29, 30].

Table 3. Vacancy migration energy and pre-factor for tracer self-diffusion

At.% Ga	Flynn E_V^m, eV	Kornblit E_V^m, eV	Flynn D_{SD}^0, m²/s	Kornblit D_{SD}^0, m²/s
0.02	0.315	0.659	2.01e-6	2.85e-6
0.034	0.313	0.685	1.99e-6	2.95e-6

Vacancy Formation Energy and Vacancy Relaxation Volume

A vacancy in a metal may be viewed as the smallest spherical void. Formation energies of nanovoids have been derived by Wolfer [3] using the concept of a surface energy that depends on the surface stress and on the electron density spill-out into the void. Taking the limit of a void containing just one vacancy, its formation energy is given by

$$\begin{aligned}
E_v^f &= 4\pi(\alpha a)^2 \gamma_0 \left[1 - (1 + \alpha a\beta / \lambda_{TF})\exp(-\alpha a\beta / \lambda_{TF})\right] \\
&\quad - 4\pi(\alpha ag)^2 / \left[\Gamma + 2\alpha aG(1 + \delta / \alpha)^{-3}\right]
\end{aligned} \tag{8}$$

and its relaxation volume by

$$V_v^{rel} / \Omega = -3\gamma_E g / \left[\Gamma + 2\alpha aG(1 + \delta / \alpha)^{-3}\right] \tag{9}$$

In these two equations,

$$\alpha = \left(\frac{3}{16\pi}\right)^{1/3} \tag{10}$$

δ = 0.477, β = 0.65, a is the lattice parameter, G is the shear modulus, and γ_0 and g are the surface energy and the surface stress for a planar surface, respectively. The surface stretch modulus can be approximated by [24]

$$\Gamma \approx 4\delta aG / (\gamma_E - 1) \tag{11}$$

where γ_E is the Eshelby factor. Its value can be determined with the elastic constants of the single crystals [25] , and to maintain consistency, the value of the isotropic shear modulus G is also evaluated with the same elastic constants according to the procedure by Gairola and Kröner [26]. Finally, we need a value for the Thomas-Fermi screening length λ_{TF} that is related to the conduction electron density. Marrouzi et al. [27] have established that this electron density correlates well with the bulk modulus B of metals as outlined in Appendix B.

The surface energy of plutonium has only been measured for the liquid state and found to be $\gamma_L = 0.55$ J/m^2. With an empirical relationship by Murr [28], the surface energy for the solid can be estimated according to

$$\gamma_0 \approx 1.2\,\gamma_L + 0.00045(T_m - T) \qquad\qquad (12)$$

where T_m is the melting temperature. At ambient temperature, $\gamma_0 \approx 1.0\,J/m^2$.

There remains then only one unknown parameter, namely the surface stress g. To obtain values for it, we use the average of measured self-diffusion energies, namely $Q_{SD} = 1.45$ eV, and subtract from it the vacancy migration energy obtained with the models by Flynn and by Kornblit. This value of the vacancy formation energy is inserted into equation (8) and solved for g. With it we compute with eq. (9) the vacancy relaxation volume.

Table 4 lists the values obtained for the two Ga-stabilized materials for which single crystal elastic constants are available [29, 30].

Table 4. Properties associated with vacancies in δ-Pu

At. % Ga	2.0	3.4
G (GPa)	16.072	16.117
Eshelby factor γ_E	1.84	1.78
a (nm)	0.46235	0.4611
λ_{TF} (nm)	0.05606	0.05583
Γ (N/m)	16.88	16.12
Flynn Vac. Formation (eV)	1.11	1.14
Kornblit Vac. Form. (eV)	0.64	0.69
Flynn g (N/m)	2.08	2.10
Kornblit g (N/m)	2.52	2.67
Flynn V_v^{rel}/Ω	-0.66	-0.60
Kornblit V_v^{rel}/Ω	-0.80	-0.76

SIA Formation, Migration, and Relaxation Volume

In the continuum mechanics treatment of a SIA, it is viewed as an elastic inclusion. A region within a homogeneous solid is assumed to undergo a transformation that

changes its density and its elastic properties from those of the surrounding unchanged material, called here the matrix. If the region before the transformation had the volume V_0, its volume after the transformation becomes greater by ΔV, and the restraining matrix now compresses this region, and the matrix is stretched in the circumferential directions. If the inclusion is a sphere, and it and the matrix are elastically isotropic, the total strain energy stored in the solid is given by

$$U = \frac{2GV_0}{3(1+\kappa\omega)}\left(\frac{\Delta V}{V_0}\right)^2 \tag{13}$$

with $\quad \omega = \frac{2(1-2\nu)}{3(1+\nu)} \quad$ and $\quad \kappa = B_I / B$ $\hfill$ (14)

Here, ν and B are the Poisson's ratio and bulk modulus of the matrix, respectively, while B_I is the bulk modulus of the inclusion.

When an extra atom is inserted into a perfect crystal region of fcc structure, and the atoms are viewed as rigid spheres, the crystal structure is expanded by 1.102 Ω [31] , where Ω is the atomic volume. However, the non-linear elastic deformation of the matrix increases this volume expansion significantly. For example, in Ni, the measured volume expansion is 1.8 Ω, indicating that the inclusion representing the SIA is under high compression and has become stiffer.
In the case of δ-Pu, it is known that the high pressure of about 330 MPa generated under the indenter of a microhardness tester induces a transformation to α-Pu [32]. This suggests that the δ-Pu atoms associated with the compressed region of a SIA are converted to α-Pu atoms.
So let us assume that the inclusion region before the insertion of an additional atom had the volume of $V_0 = n\Omega_\delta$, and it converted after the insertion to a volume of $(n+1)\Omega_\alpha$, then

$$\frac{\Delta V}{V_0} = \left(1+\frac{1}{n}\right)\frac{\Omega_\alpha}{\Omega_\delta} - 1 \tag{15}$$

Note that the ratio of the atomic volumes is $\Omega_\alpha/\Omega_\delta = 0.8$, i.e. less than one. With eq. (15) inserted into eq.(13), the strain energy becomes a function of n, $U(n)$. But this is not yet the energy of the SIA. Two other contributions must be included. The enthalpy of transformation of δ-Pu to α-Pu has been measured by Adler [33], and for $n+1$ atoms transformed, the energy released or expended is

$$\Delta H_{\delta\to\alpha}(n) = (n+1)(-4.075 + 69.04\, x_{Ga}) \quad kJ/mol\,, \tag{16}$$

Associated with the α-Pu inclusion is also an interfacial free energy of

$$F(n) = (4\pi)^{1/3} \left[3\Omega_\alpha (n+1) \right]^{2/3} \gamma_{IF} \qquad (17)$$

Unfortunately, the specific interface energy γ_{IF} between α-Pu and δ-Pu phases is not known. Typically, interface energies between different phases of the same metal are on the order of one tenth of the surface energy γ_0 for coherent interfaces to one half for incoherent interfaces [28]. The number ($n+1$) of plutonium atoms associated with a SIA can now be obtained by finding the minimum of the total energy, the sum of eqs. (13), (16), and (17):

$$E(n) = U(n) + \Delta H_{\delta \to \alpha}(n) + F(n) \qquad (18)$$

If we denote this number with n^*, then the SIA formation energy is $E(n^*)$.
We show in Fig. 2 the results obtained for the case of δ-Pu stabilized with 3.3 at.% Ga. The number of δ-Pu atoms converted to α-Pu is shown on the left, and it varies from about 2 to 4 as the interface energy decreases from 0.5 J/m² to 0.1 J/m², while the formation energy of a SIA, shown on the right, drops from 2.2 eV down to 0.5 eV.
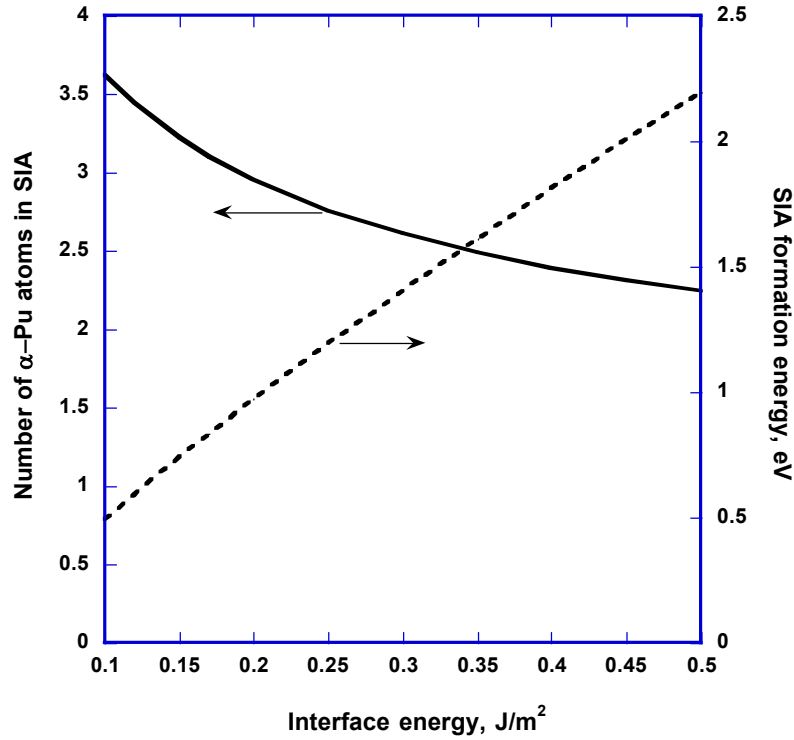

Fig. 2. Number of α-Pu atoms and SIA formation energy versus interface energy

With the number (n^*+1) of converted atoms determined, eq.(15) provides then values of the relaxation volume of SIA; they are displayed in Fig. 3 .

We note that an inclusion formed by five α-Pu atoms, one atom inserted into four matrix atom of initial volume $4\Omega_\delta$, produces no misfit, hence zero relaxation volume and zero strain energy. But even the conversion of fewer atom results in relaxation volumes below $0.5\Omega_\delta$, of about the same magnitude as the absolute value of the vacancy relaxation volume. This implies that there exists no significant preference for SIA absorption at dislocations in δ-Pu.

The SIA formation energy predicted is also much lower than in other fcc metals, and it is similar in magnitude to the activation energy for self-diffusion.

The change in the atomic volume from Ω_δ to Ω_α has been explained by more 5f electrons becoming itinerant. The formation of a SIA in the present model is then associated with electronic transitions that render it a dynamic defect, and the effective number of α-Pu atom in it need not be a fixed integer. Migration of this defect may then be viewed as follows. A δ-Pu atom adjacent to the SIA releases in response to a large thermal fluctuation a 5f electron and in the process becomes a smaller α-Pu atom. However, the released 5f electron is captured by one of the α-Pu atoms in the SIA, and it converts to a δ-Pu atom. The number of α-Pu atoms remains the same as before, but the SIA has moved its center of mass. During this transition the SIA energy reached temporarily the value of *E(n*+1).*
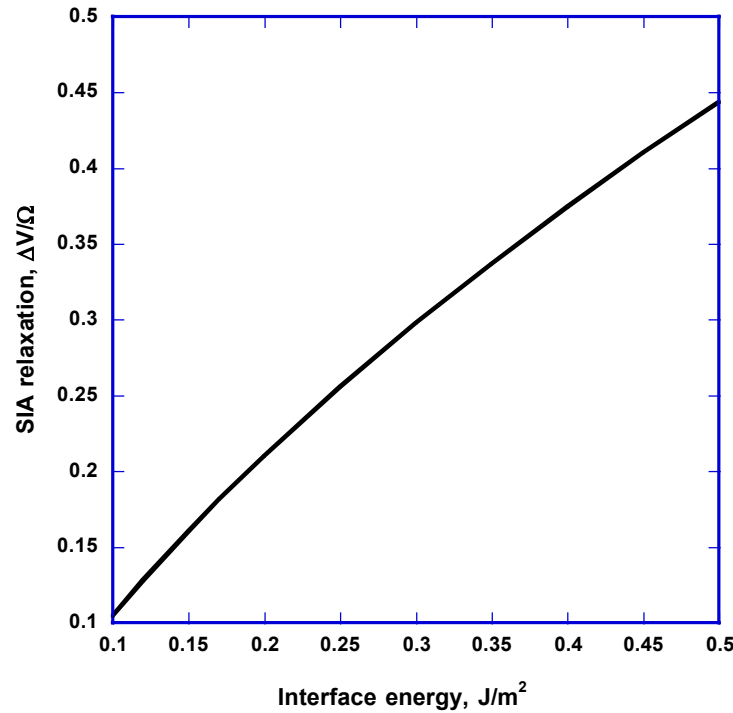

Fig. 3. SIA relaxation volume as a function of the interface energy

Hence, the activation energy for SIA migration can be obtained from

$$E_{SIA}^{m}(n*) = E(n*+1) - E(n*) \tag{19}$$

This migration energy is shown in Fig. 4 as a function of (*n*+1*) together with the formation energy. It is seen that the migration energy is about one tenth of the formation energy for any possible value of the interfacial energy. Migration energies of this magnitude have also been found for regular fcc metals.
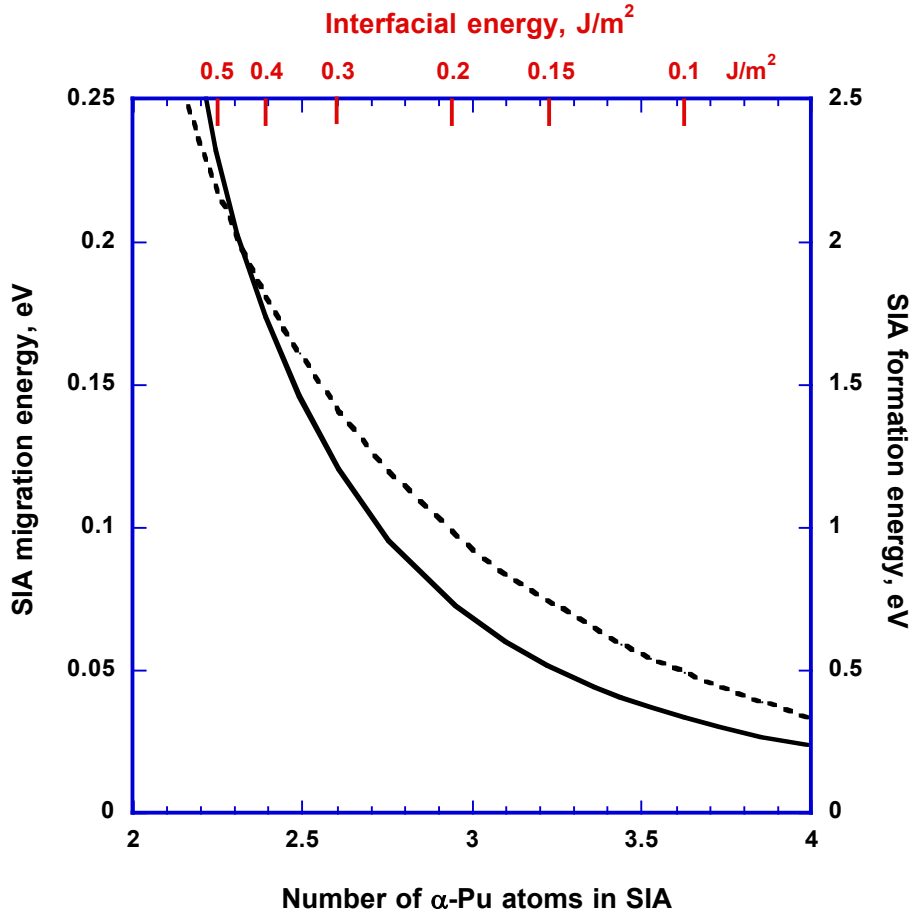

Fig. 4. SIA migration and formation energies as a function of the number of atoms contained in it. The top scale shows associated interface energy.

Conclusions

For a better overview we list in Table 5 the ranges of values predicted by the three different methods for the properties of vacancies and SIA in δ-Pu. Lowest and highest values are selected for a particular property obtained with a particular method to define the range. When values for the self-diffusion energy or for the sum of SIA formation and migration are given, both parts had to appear together in the same publication. However, self-diffusion energies listed under CM are in fact published experimental values, and their average of 1.45 eV was used to obtain vacancy formation energies with the CM method.

Table 5. Ranges for defect properties predicted with different methods. Energies are in units of eV/atom. Numbers in brackets are experimental values.

	MEAM	DFT	CM
E_V^f	0.44 ~ 0.58	1.08 ~ 1.75	0.64 ~ 1.14
E_V^m	0.80 ~ 1.29	0.56 ~ 0.85	0.31 ~ 0.69
$E_V^f + E_V^m = Q_{SD}$	1.24 ~ 1.87	1.76 ~ 2.35	(1.03 ~ 1.74)
E_{SIA}^f	0.49 ~ 1.16	0.73 ~ 0.80	0.49 ~ 2.2
E_{SIA}^m	0.056 ~ 0.4		0.033 ~ 0.23
$E_{SIA}^f + E_{SIA}^m$	0.57 ~ 1.56		0.525 ~ 2.43
$-V_V^{rel}/\Omega_\delta$		0.62 ~ 0.95	0.60 ~ 0.80
$V_{SIA}^{rel}/\Omega_\delta$		0.40 ~ 1.40	0.10 ~ 0.44

Vacancy formation energies predicted with DFT seem to be too large by a factor of two, although vacancy migration energies appear to be more reasonable. Both MEAM and CM predict a wide range of vacancy migration energies, but the highest value from MAEM is too close to the average experimental value for self-diffusion. Vacancy migration energies predicted with the models by Flynn and by Kornblit for normal fcc metals give similar values that are in good agreements with experimental values. It is then surprising that when applied to δ-Pu, the Flynn model predicts a very low value of 0.31 eV, while the Kornblit model generates a value of 0.69 eV, about half the self-diffusion energy; this partitioning is in fact the rule for normal fcc metals.

Perhaps the most surprising result is the low values predicted for the SIA formation energy with all three methods. When migration energies are also predicted, the sum $E_{SIA}^f + E_{SIA}^m$ has a range from 0.57 to 1.56 eV for MEAM, and from 0.53 to 2.4 eV for CM calculations, and these ranges overlap with those for self-diffusion energies. It raises the possibility that both vacancies and SIA can be created by thermal activation in δ-Pu. To

put this in perspective, it is instructive to compare δ-Pu with Al. Resistivity recovery experiments on aluminum gave a value of 3.3 ± 0.6 eV for $E_{SIA}^f + E_{SIA}^m$ [35], much larger than its self-diffusion energy of 1.28 eV.

Relaxation volumes predicted for vacancies and SIA in δ-Pu are also quite different than measured values in normal fcc metals. In these metals, the vacancy relaxation volume is between -0.2 Ω and -0.3 Ω, and the SIA relaxation volume is between 1.5 Ω and 1.8 Ω. In contrast, vacancies in δ-Pu are predicted to have large negative values from -0.6 Ω to -0.95 Ω, while SIA possess small relaxation volumes, of the same order of magnitude or even smaller than the absolute values of the relaxation volumes for vacancies. This implies that vacancies may be attracted to dislocations more than SIA, and the fundamental mechanism for radiation-induced void swelling is absent in δ-Pu.

DFT calculations with spin polarization have been very successful to explain and predict the different allotropes of plutonium. It is then disappointing that predicted properties for vacancies and for SIA in δ-Pu are still questionable. As a next step, it may be worthwhile to first explore what DFT with spin polarization will predict for a crystal containing both phases, α-Pu and δ-Pu.

Appendix A. Evaluation of the Eshelby Factor

The evaluation of strain fields for defects in anisotropic materials makes use of the elastic Green's function. While this Green's function can be represented in analytic form in reciprocal space, in real space analytical forms exist only for isotropic and hexagonal crystals. The strategy adopted for anisotropic materials has been to define an appropriate isotropic approximation and to treat the deviations from isotropy by either perturbation theory or by variational methods. Both of these approaches have been studied and utilized by Leibfried and Breuer [25]. In particular, we use their results to establish a analytical correlation. For it we make use of the anisotropy constant

$$C_A = C_{11} - C_{12} - 2 C_{44},$$ (A1)

the bulk modulus

$$B = (C_{11} + 2 C_{12}) / 3,$$ (A2)

and the two Voigt constants

$$\overline{C}_{11} = C_{11} - 2 C_A / 5$$ (A3)

$$\overline{C}_{44} = C_{44} + C_A / 5$$ (A4)

Leibfried and Breuer [25] have computed the Eshelby factor for many metals and found that it is determined by two constants, namely by the ratios of

$\overline{C}_{11}/B$ and $C_A/\overline{C}_{44}$. We are able to fit their numerical results to the following expression

$$\gamma_E = \frac{\overline{C}_{11}}{B}\left[1 + 0.002458\left(\frac{C_A}{\overline{C}_{44}}\right)^4\right]^{(-1)} \tag{A5}$$

Using the elastic constants of Ledbetter and Moment [30] and those of Wong et al. [29] determined from phonon dispersion measurements, we obtain the Eshelby factors listed in the last column of Table A1.

Table A1. Elastic Constants for δ-Pu in units GPa and Eshelby Factors

Ref.	C_{11}	C_{12}	C_{44}	B	C_A	$C_A/\overline{C}_{44}$	$\overline{C}_{11}/B$	γ_E
30	36.28	26.73	33.59	29.91	-57.6	-2.610	1.983	1.78
29	35.3	23.9	30.6	27.27	-51.1	-2.507	1.997	1.84

Appendix B. Correlation between Bulk Modulus and Free Electron Density

The connection between the free electron density or Wigner-Seitz parameter and the bulk modulus is shown in Fig. B1, a reproduction of a similar figure in Ref. [27]. If n_e denotes the number of free electrons per atom, then

$$r_s/a_B = \left(\frac{3}{4\pi n_e}\right)^{1/3} \tag{B1}$$

where a_B is the Bohr radius. The data can be fitted to the power law

$$B(GPa) = 3120.3(r_S/a_B)^{-4.607} = 28157\, n_e^{1.536} \tag{B2}$$

For the bulk modulus of δ-Pu, 28 GPa, one obtains a free electron density of 0.011 per atom, or 1.04 of the 94 electrons in an atom. This agrees with electronic structure calculations that show that one of the 5f electrons is itinerant in δ-Pu. For α-Pu with a bulk modulus of 55 GPa, 1.62 of the 5f electrons are de-localized. The Thomas-Fermi screening length is defined as [34]

$$\lambda_{TF} = a_B\left(\frac{\pi}{12}\right)^{1/3}\sqrt{\frac{r_S}{a_B}} \tag{B3}$$

and it can therefore also be related to the bulk modulus using eq. (B2). We obtain

$$\lambda_{TF}(nm) = 0.081 \left[B(GPa) \right]^{-0.1085} \tag{B4}$$
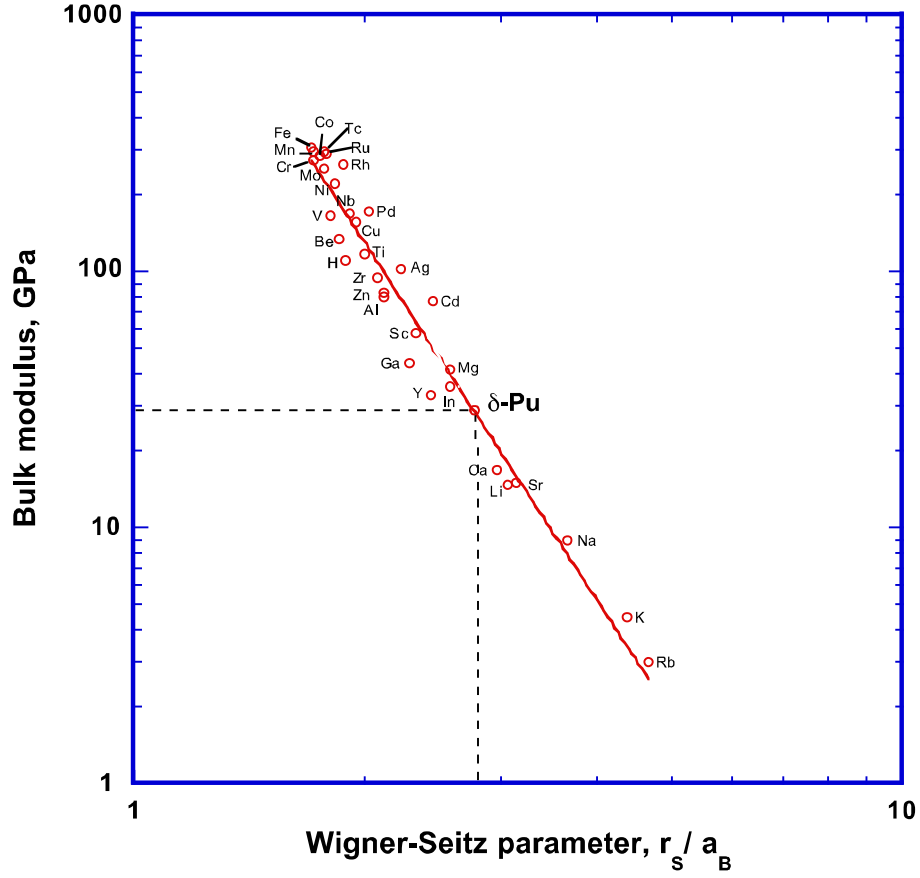
and λ_{TF} = 0.05646 nm for δ-Pu.

Fig. B1. Correlation between bulk modulus and Wigner-Seitz parameter for metals [27].

References

1. A.J. Schwartz, M.A. Wall, T.G. Zocco, W.G. Wolfer, Phil. Mag. 85 (2005) 479
2. P.H. Dederichs, C. Lehmann, H.R. Schober, A. Scholz, R. Zeller, J. Nucl. Mater. 69 & 70 (1978) 176
3. W.G. Wolfer, Fundamental Properties of Defects in Metals, in Comprehensive Nuclear Materials, ed. R.I.M. Konings, Vol. 1, chapter1, Elsevier, 2012
4. M.I. Baskes, Phys. Rev. B62 (2000) 15532
5. M.I. Baskes, S.P. Chen, F.J. Cherne, Phys. Rev. B66 (2002) 104107
6. S.M. Valone, M.I. Baskes, R.L. Martin, Phys. Rev. B73 (2006) 214209
7. S.M. Valone, M.I. Baskes, M. Stan, T.E. Mitchell, A.C. Lawson, K.E. Sickafus, J. Nucl. Mater. 324 (2004) 41
8. B.P. Uberuaga, S.M. Valone, J. Nucl. Mater. 375 (2008) 44
9. 4. V.V. Dremov, A.V. Karavaev, S.I. Samarin, F.A. Sapozhnikov, M.A. Zocher, D.L. Preston, J. Nucl. Mater. 385 (2009) 79-82
10. L. Berlu, G. Jomard, G. Rosa, P. Faure, J. Nucl. Mater. 372 (2008) 171
11. B. Ao, X. Wang, W. Hu, J. Yang, Phys. Stat. Sol. (b) 245 (2008) 1493
12. M. Robinson, S.D. Kenny, R. Smith, M.T. Storr, E. McGee, Nucl. Inst. Meth. B267 (2009) 2967
13. M. Robinson, S.D. Kenny, R. Smith, M.T. Storr, J. Nucl. Mater. 423 (2012) 16, J. Nucl. Mater. 444 (2014) 493
14. G. Robert, A. Pasturel, B. Siberchicot, J. Alloys Compounds 444-445 (2006) 191
15. G. Robert, A. Pasturel, B. Siberchicot, Europhys. Lett. 71 (2005) 412
16. B. Sadigh, J. Sturgeon, W.G. Wolfer, MRS presentation (2005)
17. B. Sadigh, JASON Pitlife study, Jan. 2005
18. B. Sadigh, private communication, July 2014
19. P. Söderlind, private communication
20. C.P. Flynn, Phys. Rev. 171 (1968) 682; Phys. Rev. 179 (1969) 920
21. P. Ehrhart, K.-H. Robrock, H.R. Schober, Physics of Radiation Effects in Crystals, eds. R.A. Johnson, A.N. Orlov, Elsevier, 1986, chapter 1
22. L. Kornblit, J. Pelleg, A. Rabinovitch, Phys. Rev. 16 (1977) 1164
23. A. Seeger, H. Mehrer, Vacancies and Interstitials in Metals, eds. A. Seeger, D. Schumacher, W. Schilling, J. Diehl, North-Holland, 1970, p. 1
24. W.G. Wolfer, Acta Materialia 59 (2011) 7736
25. G. Leibfried, N. Breuer, Point Defects in Metals, Springer Tracts in Modern Physics 81, 1978
26. B.K.D. Gairola, E. Kröner, Int. J. Eng. Sci. 19 (1981) 865
27. V.L. Moruzzi, J.F. Janak, A.R. Williams, Calculated Electronic Properties of Metals, Pergamon Press, 1978, p. 26
28. L.E. Murr, Interfacial Phenomena in Metals and Alloys, Addison-Wesley, 1975
29. J. Wong et al., Phys. Rev. B72 (2005) 064115
30. H.M. Ledbetter, R.L. Moment, Acta Met. 24 (1976) 891
31. W.G. Wolfer, J. Phys. F: Met. Phys. 12 (1982) 425
32. R.A. Pereyra, Materials Characterization 59 (2008) 1675

33. P.H. Adler, Metall. Trans. 22A (1991) 2237
34. C. Kittel, Quantum Theory of Solids, 2nd ed., Wiley & Sons, 1987, p. 112
35. W. Schilling, J. Nucl. Mater. 69 & 70 (1978) 465